# Prediction of dissolved oxygen in urban rivers at the Three Gorges Reservoir, China: extreme learning machines (ELM) versus artificial neural network (ANN)

Senlin Zhu and Salim Heddam

## ABSTRACT

In the present study, two non-linear mathematical modelling approaches, namely, extreme learning machine (ELM) and multilayer perceptron neural network (MLPNN) were developed to predict daily dissolved oxygen (DO) concentrations. Water quality data from four urban rivers in the backwater zone of the Three Gorges Reservoir, China were used. The water quality data selected consisted of daily observed water temperature, pH, permanganate index, ammonia nitrogen, electrical conductivity, chemical oxygen demand, total nitrogen, total phosphorus and DO. The accuracy of the ELM model was compared with the standard MLPNN using several error statistics such as root mean squared error, mean absolute error, the coefficient of correlation and the Willmott index of agreement. Results showed that the ELM and MLPNN models perform well for the Wubu River, acceptably for the Yipin River and moderately for the Huaxi River, while poor model performance was obtained at the Tributary of Huaxi River. Model performance is negatively correlated with pollution level in each river. The MLPNN model slightly outperforms the ELM model in DO prediction. Overall, it can be concluded that MLPNN and ELM models can be applied for DO prediction in low-impacted rivers, while they may not be appropriate for DO modelling for highly polluted rivers.

**Key words** | artificial neural network, dissolved oxygen, extreme learning machines, Three Gorges Reservoir, water quality

**Senlin Zhu** (corresponding author)
State Key Laboratory of Hydrology-Water Resources and Hydraulic Engineering,
Nanjing Hydraulic Research Institute,
Nanjing 210029,
China
E-mail: *slzhu@nhri.cn*

**Salim Heddam**
Faculty of Science, Agronomy Department,
Hydraulics Division, Laboratory of Research in Biodiversity Interaction Ecosystem and Biotechnology,
University 20 Août 1955,
Route El Hadaik, BP 26, Skikda,
Algeria

*This article has been made Open Access thanks to the kind support of CAWQ/ACQE (https://www.cawq.ca).*

## INTRODUCTION

Dissolved oxygen (DO) is an essential resource of aquatic ecosystems. The DO concentration plays a critical role in regulating various biogeochemical processes and biological communities in rivers. DO concentrations can fluctuate over the day and night in response to climate changes and the respiratory requirements of aquatic plants (Heddam 2014a). Aquatic organisms are sensitive to fluctuations of DO levels in water bodies, especially for DO reductions. Severe oxygen depletion can lead to fish kills (Meding & Jackson 2003; Robarts *et al.* 2005), and changes in community composition and trophic state (Wetzel 2001; Ruuhijärvi *et al.* 2010; Branco *et al.* 2016). The overall DO concentrations in a river are balanced by re-aeration at the water surface, primary production by photosynthesis and consumptions by biochemical oxygen demands in the water column or sediment oxygen demand (Poulson & Sullivan 2010).

Due to the complexity of factors impacting DO levels, it is important to understand how these factors determine the level of oxygen available for living organisms, and prediction of DO concentrations is crucial for aquatic managers responsible for the maintenance of ecosystem health (Meding & Jackson 2003). Mathematical models provide useful tools to predict the spatio-temporal dynamics of DO



doi: 10.2166/wqrj.2019.053

in water bodies. Many sophisticated deterministic models have been developed in the past years to predict DO levels in rivers, such as QUAL2E, QUAL2 K and WASP (Cox 2003; Kannel *et al.* 2010). These mechanistic computer softwares can simulate processes which impact DO levels, such as hydrodynamics, dispersion and pollutant kinetics in the natural environment. These models have been widely used in different river systems, such as applications of the QUAL2E model in the Corumbataí River (Palmieri & Carvalho 2006) and Putzu River (Yang *et al.* 2011), and DO simulations with the QUAL2 K model (Du *et al.* 2008; Cho & Ha 2010). Generally, many input data are needed to run these models, such as topography, flow discharge and water level, water quality concentrations and meteorological data. The highly intensive data need sometimes limit the applications of these mechanistic models.

Except for the mechanistic models, there has been a widespread interest in the application of artificial intelligence techniques for DO modelling in water bodies, such as the artificial neural network (ANN)-based approach (Soyupak *et al.* 2003; Schmid & Koskiaho 2006; Diamantopoulou *et al.* 2007; Singh *et al.* 2009; Chen *et al.* 2010; Ay & Kisi 2012; Wen *et al.* 2013; Antanasijević *et al.* 2013; Heddam 2014a; Keshtegar & Heddam 2017; Csábrági *et al.* 2017), fuzzy logic models (Altunkaynak *et al.* 2005; Giusti & Marsili-Libelli 2009; Zounemat-Kermani & Scholz 2014), neurofuzzy models (Heddam 2014b; Najah *et al.* 2014; Ay & Kisi 2017), support vector machine models (Li *et al.* 2013; Liu *et al.* 2013; Ji *et al.* 2017; Heddam & Kisi 2018) and extreme learning machine (ELM) models (Heddam 2016; Heddam & Kisi 2017). These approaches use available water quality parameters, such as water temperature, pH, electrical conductivity (EC) as inputs. Various ANN models have been developed, and the most reported models are the multilayer perceptron neural networks (MLPNN) (Schmid & Koskiaho 2006; Ay & Kisi 2012; Wen *et al.* 2013; Keshtegar & Heddam 2017). Recently, Heddam (2016) and Heddam & Kisi (2017) proposed a new approach (ELM) to model DO concentrations in water bodies. The proposed ELM models were applied in eight rivers in the US for estimating DO using four water quality variables as inputs (water temperature, turbidity, pH and EC). In this study, the ELM model was applied in four urban rivers in the Three Gorges Reservoir (TGR) region, China, and model performance was compared with the MLPNN approach. The main objective of this study is to develop models which can be used to inform water quality management for one of the largest reservoirs in the world (TGR).

## MATERIALS AND METHODS

### Study area and data set

The Yangtze River is the largest river in China and the third largest in the world. The TGR is located at the end of the upper Yangtze River. It is one of the largest man-made reservoirs in the world with a surface area of 1,084 $km^2$, a storage capacity of 39.3 billion $m^3$ and a watershed area larger than 1 million $km^2$ (Wang *et al.* 2005). Four urban tributaries in Chongqing City, located in the terminal of the backwater zone of the TGR, were studied in this paper. Observed data from ten monitoring stations in these four rivers were used in the water quality analysis (Table 1).

The Wubu River is listed as a water source protection area for centralized drinking water supply, thus its water

**Table 1** | Characteristics of the studied rivers

| River | Length (km) | Watershed area ($km^2$) | Annual flow rate ($m^3/s$) | Monitoring stations and data sets |
|---|---|---|---|---|
| Yipin | 51.0 | 363.0 | 5.28 | 3 (CSZ, BJDK, YHQ from upstream to downstream), 108 data points |
| Huaxi | 63.62 | 268.46 | 3.6 | 3 (NHCK, JLY, SLQ from upstream to downstream), 108 data points |
| Wubu | 84.4 | 871.0 | 13.11 | 2 (JQ, ZC from upstream to downstream), 72 data points |
| Tributary of Huaxi River | 8.5 | 54.5 | / | 2 (CS1, CS2 from upstream to downstream), 72 data points |

quality conditions are good generally (DO: 6.1–10.0). The Huaxi river basin is mainly an urban watershed where large and medium-sized enterprises and agricultural crop areas are densely distributed. In recent years, the population in the Huaxi basin has increased rapidly. Excessive household and municipal sewage, industrial wastewater and agricultural fertilizers contribute greatly to water pollution in the Huaxi River (DO: 2.9–10.0, COD: 10.0–39.0, TN: 0.69–8.17). The water quality conditions of the tributary of the Huaxi River are the poorest among all the rivers due to excessive household and municipal sewage (DO: 0.4–7.8, COD: 13.1–156.0, TN: 5.03–41.4). The Yipin River was also impacted by anthropogenic activities in recent years, and its water quality conditions are poor as well (DO: 5.2–10.5). Water quality assessment results indicated that Tributary of Huaxi River > Huaxi River > Yipin River > Wubu River for pollution level (Zhu *et al.* 2018). Water quality data sets used were in the period from 2013 to 2015, with one sampling per month. Water quality parameters include water temperature (TE), pH, DO, permanganate index (PI), $NH_3$-N, EC, chemical oxygen demand (COD), total nitrogen (TN) and total phosphorus (TP). The statistical summary of the used data sets for all rivers are summarized in Table 2. According to the statistical indices reported in Table 2, the data are not homogenous and there is a large variability trend among the water quality variables. Except for water temperature and pH, for which the variability is not noticeable, it is clear from Table 2 that the Yangtze River and its tributaries result in a nonhomogeneous data set, especially for EC, TN, TP and PI. The biological variables (DO and COD) are the same, as shown by the mean, max and min values in Table 2. The high values of COD along the Tributary of Huaxi River indicate that the river receives highly non-biodegradable organic matter. The findings suggest the potential and substantial variability in water quality data across the four rivers, especially between the Tributary of Huaxi River and the other three rivers. The data set for the four rivers was divided into two sub-data sets: (i) training subset (70%) and (ii) validation subset (30%).

Generally, DO in all rivers negatively correlated with TE, and with the increase of pollution level, the coefficient of correlation ($R$) decreased (Table 2). Additionally, DO presented poor correlations with other water quality parameters (Table 2). All the input water quality variables and DO were standardized using the Z-score method (Olden & Jackson 2002):

$$Z_n = \frac{x_n - x_m}{\sigma_x} \tag{1}$$

where $Z_n$ is the normalized value of the observation $n$, $x_n$ is the measured value of the observation $n$, $x_m$ and $\sigma_x$ are the mean value and standard deviation of the variable $x$. In the present study, we evaluated several combinations of the water quality variables based on the correlations between water quality variables and DO and, in total, nine scenarios were compared (Table 3).

## Multilayer perceptron neural network (MLPNN)

ANN and their several algorithms have played a critical role in modelling, forecasting and classifying water quality variables. The availability of large data sets and the increase of monitoring stations worldwide will continue to encourage the use of ANN models in several areas of environmental science. One of the principal advantages that have potentially increased the applications of ANN models is that they do not make any assumption about the structure of the data set, and the models are developed based on training algorithm. ANN is a special kind of non-linear model, proposed and inspired by the function of the human brain. The term network refers to a system of interconnected nodes or neurons, similar to biological neurons (Haykin 1999). Generally, the ANN models have three kinds of layers: (i) input layer that contains the water quality variables selected for developing the DO model (reported as $x_i$), (ii) one or more hidden layers and (iii) the output layer, having only the dependent variable (the DO concentration reported as $y$). If the interconnection between the neurons is unidirectional, such an ANN model is called feed-forward neural network (FFNN).

The most widely used FFNN model is the multilayer perceptron neural network (Rumelhart *et al.* 1986), which generally is composed of only one hidden layer in addition to the input and output layers, and has been reported in the literature as universal approximators (Hornik *et al.* 1989; Hornik 1991). The neurons in the hidden layers are

**Table 2** | Statistical summary of the used data sets for all rivers

| Variables | Unit | $X_{mean}$ | $X_{max}$ | $X_{min}$ | $S_x$ | $C_v$ | $R$ |
|---|---|---|---|---|---|---|---|
| Yipin River | | | | | | | |
| TE | °C | 19.551 | 32.000 | 8.000 | 6.785 | 0.347 | −0.703 |
| pH | / | 7.688 | 8.090 | 7.200 | 0.196 | 0.026 | −0.112 |
| EC | μS/cm | 398.299 | 734.800 | 207.800 | 123.246 | 0.309 | 0.166 |
| $NH_3$-N | mg/L | 0.527 | 1.870 | 0.121 | 0.384 | 0.728 | −0.020 |
| TN | mg/L | 2.344 | 4.030 | 0.930 | 0.777 | 0.332 | −0.161 |
| TP | mg/L | 0.100 | 0.234 | 0.051 | 0.029 | 0.289 | −0.241 |
| PI | mg/L | 3.727 | 6.100 | 2.400 | 0.623 | 0.167 | −0.211 |
| COD | mg/L | 13.634 | 23.800 | 10.000 | 3.216 | 0.236 | −0.017 |
| DO | mg/L | 7.637 | 10.500 | 5.200 | 1.101 | 0.144 | 1.000 |
| Huaxi River | | | | | | | |
| TE | °C | 19.050 | 33.000 | 7.000 | 7.011 | 0.368 | −0.372 |
| pH | / | 7.752 | 8.640 | 7.170 | 0.232 | 0.030 | 0.261 |
| EC | μS/cm | 508.050 | 962.700 | 144.300 | 208.893 | 0.411 | −0.265 |
| $NH_3$-N | mg/L | 1.315 | 2.290 | 0.172 | 0.725 | 0.551 | −0.490 |
| TN | mg/L | 3.697 | 8.170 | 0.690 | 2.134 | 0.577 | −0.500 |
| TP | mg/L | 0.182 | 0.415 | 0.016 | 0.130 | 0.715 | −0.516 |
| PI | mg/L | 5.203 | 7.800 | 2.000 | 0.913 | 0.175 | −0.352 |
| COD | mg/L | 18.787 | 39.000 | 10.000 | 6.246 | 0.332 | −0.032 |
| DO | mg/L | 6.998 | 10.000 | 2.900 | 1.216 | 0.174 | 1.000 |
| Wubu River | | | | | | | |
| TE | °C | 19.482 | 34.000 | 8.000 | 7.083 | 0.364 | −0.751 |
| pH | / | 7.708 | 8.190 | 6.350 | 0.289 | 0.037 | 0.127 |
| EC | μS/cm | 434.368 | 938.000 | 202.000 | 142.466 | 0.328 | 0.452 |
| $NH_3$-N | mg/L | 0.300 | 0.846 | 0.108 | 0.134 | 0.447 | −0.248 |
| TN | mg/L | 1.378 | 3.220 | 0.810 | 0.598 | 0.434 | −0.122 |
| TP | mg/L | 0.076 | 0.197 | 0.044 | 0.024 | 0.316 | −0.420 |
| PI | mg/L | 3.089 | 4.700 | 1.100 | 0.676 | 0.219 | −0.399 |
| COD | mg/L | 11.933 | 18.300 | 10.000 | 1.891 | 0.158 | −0.132 |
| DO | mg/L | 7.938 | 10.000 | 6.100 | 1.008 | 0.127 | 1.000 |
| Tributary of Huaxi River | | | | | | | |
| TE | °C | 19.069 | 35.000 | 9.000 | 6.535 | 0.343 | −0.358 |
| pH | / | 7.710 | 8.090 | 7.420 | 0.150 | 0.020 | 0.004 |
| EC | μS/cm | 905.883 | 1,241.700 | 577.000 | 137.632 | 0.152 | 0.198 |
| $NH_3$-N | mg/L | 7.297 | 25.400 | 1.100 | 5.488 | 0.752 | −0.252 |
| TN | mg/L | 14.027 | 41.400 | 5.030 | 9.542 | 0.680 | −0.305 |
| TP | mg/L | 0.783 | 2.740 | 0.153 | 0.457 | 0.583 | 0.070 |
| PI | mg/L | 9.044 | 32.300 | 4.100 | 5.194 | 0.574 | −0.327 |
| COD | mg/L | 42.097 | 156.000 | 13.100 | 30.629 | 0.728 | −0.212 |
| DO | mg/L | 4.002 | 7.800 | 0.400 | 1.765 | 0.441 | 1.000 |

$X_{mean}$, mean; $X_{max}$, maximum; $X_{min}$, minimum; $S_x$, standard deviation; $C_v$, coefficient of variation; $R$, coefficient of correlation with DO, TE, water temperature, EC, specific conductance, $NH_3$-N, ammonia nitrogen, TN, total nitrogen, TP, total phosphorus, PI, permanganate index, COD, chemical oxygen demand, DO, dissolved oxygen; °C, Celsius; μS/cm, micro Siemens per centimetre; mg/L, milligram per litre.

**Table 3** | The input combinations of different models

| Models | | |
|---|---|---|
| **MLPNN** | **ELM** | **Inputs combinations** |
| MLPNN1 | ELM1 | TE, pH, PI, EC, TP, $NH_3$-N, TN, COD |
| MLPNN2 | ELM2 | TE, EC, TP, $NH_3$-N, TN |
| MLPNN3 | ELM3 | pH, PI, EC, $NH_3$-N, TN |
| MLPNN4 | ELM4 | TE, pH, EC, $NH_3$-N, TP |
| MLPNN5 | ELM5 | EC, $NH_3$-N, TP, TN |
| MLPNN6 | ELM6 | TE, PI, EC, $NH_3$-N |
| MLPNN7 | ELM7 | TE, PI, EC, TP |
| MLPNN8 | ELM8 | TE, EC, TP |
| MLPNN9 | ELM9 | TE, PI, EC |

ELM, extreme learning machines; MLPNN, multilayer perceptron neural network.

the most important component of the MLPNN model, and they play dual roles: (i) receiving signals from the input layers (the $x_i$) and calculating a weighted sum by multiplying each input variable ($x_i$) with a weight term ($w_i$), adding a bias term ($\delta_i$) and (ii) passing the sum via an activation function to the neuron in the next layer. The unique neuron in the output layer plays the same role as the neuron in the hidden layer, except that its activation function is generally the identity (linear). The number of neurons in the hidden layer are proceeded by trial and error. Determination of the optimal set of weights and biases of the MLPNN model is the most important task that must be achieved using the backpropagation (BP) algorithm. During this process, the weights and biases are updated to minimize a cost function, generally the mean square error (MSE) (Haykin 1999). MLPNN with one hidden layer contains $n$ neurons and one output layer with only one neuron, expressed as follows (Figure 1):

$$Y = f_2\left[\sum_{j=1}^{n} w_{jk}\left[f_1\left(\sum_{j=1}^{n} x_i w_{ij} + \delta_j\right)\right] + \delta_0\right] \quad (2)$$

where $x_i$ is the input variable, $w_{ij}$ is the weight between the input $i$ and the hidden neuron $j$, $\delta_j$ is the bias of the hidden neuron $j$, $f_1$ the activation sigmoid function, represented by Equation (3), $w_{jk}$ is the weight of connection of neuron $j$ in the hidden layer to unique neuron $k$ in the output layer; $\delta_0$ is the bias of the output neuron $k$, and finally

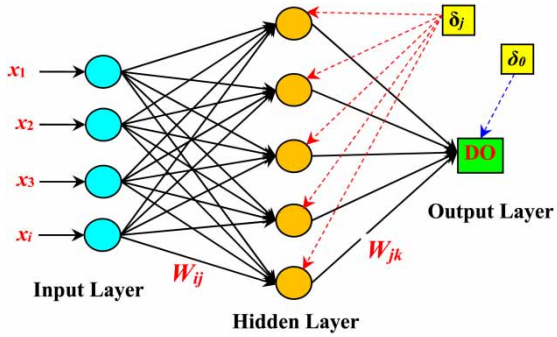


**Figure 1** | Multilayer perceptron neural network (MLPNN) architecture.

$f_2$ is a linear activation function for the neuron in the output layer:

$$f_1(x) = \frac{1}{1+e^{-x}} \quad (3)$$

## Extreme learning machines (ELM)

As stated earlier in the description of the MLPNN model, during the training process, the matrices of weights and biases must be updated, and consequently, the complexity of the model increases with the increase of the number of neurons in the hidden and input layers. One of the most important algorithms proposed during the last decade for training the MLPNN model is the ELM model introduced by Huang *et al.* (2006a, 2006b), for single layer feed-forward neural network (SLFN). Contrary to the SLFN in which the weights between the input and the hidden layer ($W_{ij}$, Figure 1) are determined iteratively using the BP algorithm, they are randomly initialized and fixed using the ELM. Regarding the weights between the hidden and output layers ($W_{jk}$, Figure 1), they are optimized by solving the Moore–Penrose generalized inverse of matrix (Huang et al. 2006a, 2006b).

Let us consider two set of variables, dependent $y_i$ and independent $x_i$ which comprises a training data set $\{x_i, y_i\}$, $i = 1, \ldots, N$, in which, $x_i \varepsilon R^d$ and $y_i \varepsilon R^c$, the ELM with L hidden neuron can be expressed as:

$$y_i = f_L(x_i) = \sum_{j=1}^{L} \beta_j h_j(x_i) = h(x_i)\beta \quad (4)$$

where $\beta_j$ is a weight vector connecting the $j$th hidden neuron and the output neurons, and $h(x) = [h_1(x), \ldots, h_L(x)]$ is the

output vector of the hidden layer with respect to the input $x$, which maps the data from input space to the ELM feature space. Similar to the SLFN, several activations' functions can be used for the ELM, among them the sigmoidal, hard-lim, triangular and radial basis. The N equations coming from Equation (4) can be written in a compact form and are represented by $H\beta = Y$, where H is the hidden layer output matrix. The weights connecting the hidden layer and the output layers, denoted by $\beta$, are achieved by minimal norm least square method (Wei *et al.* 2015; Yan *et al.* 2017; Zhang *et al.* 2018):

$$\beta = H^{+}Y \tag{5}$$

where $H^{+}$ is the Moore–Penrose generalized inverse of matrix H (Huang *et al.* 2006a, 2006b). For applying the ELM models, we used the Matlab codes available at http://www.ntu.edu.sg/ home/egbhuang/elm_codes.html.

### Performance assessment of the models

In this study, model performance was evaluated using the following statistical indices metrics: the coefficient of correlation ($R$), the Willmott index of agreement ($d$), the root mean squared error ($RMSE$) and the mean absolute error ($MAE$):

$$R = \left[ \frac{\frac{1}{\mathrm{N}} \sum (\mathrm{O}_i - \mathrm{O}_m)(\mathrm{P}_i - \mathrm{P}_m)}{\sqrt{\frac{1}{\mathrm{N}} \sum_{i=1}^{n} (\mathrm{O}_i - \mathrm{O}_m)^2} \sqrt{\frac{1}{\mathrm{N}} \sum_{i=1}^{n} (\mathrm{P}_i - \mathrm{P}_m)^2}} \right] \tag{6}$$

$$d = 1 - \frac{\sum_{i=1}^{N} (\mathrm{P}_i - \mathrm{O}_i)^2}{\sum_{i=1}^{N} (|\mathrm{P}_i - \mathrm{O}_m| + |\mathrm{O}_i - \mathrm{O}_m|)^2} \tag{7}$$

$$RMSE = \sqrt{\frac{1}{\mathrm{N}} \sum_{i=1}^{\mathrm{N}} (\mathrm{O}_i - \mathrm{P}_i)^2} \tag{8}$$

$$MAE = \frac{1}{N} \sum_{i=1}^{N} |\mathrm{O}_i - \mathrm{P}_i| \tag{9}$$

where $N$ is the number of data points, $O_i$ is the measured and $P_i$ is the corresponding model prediction of dissolved oxygen concentrations. $O_m$ and $P_m$ are the average values of $O_i$ and $P_i$.

## RESULTS AND DISCUSSION

In the following, we assess the capability and usefulness of the MLPNN and ELM models for predicting DO concentrations at four rivers in China, using eight water quality variables as predictors (TE, pH, PI, EC, TP, $NH_3$-N, TN and COD). To prevent overfitting, cross-validation is conducted for both models. The estimated values of the performance indices in the training and validation phases are shown in Tables 4–7, respectively. As a preliminary analysis, results obtained show that the ELM and MLPNN models perform well for the Wubu River, acceptably for the Yipin River, moderately for the Huaxi River, and poorly for the Tributary of Huaxi River in DO prediction. This can be explained by considering that: (i) model performance is negatively correlated with pollution level in each river, (ii) the MLPNN and ELM models can be applied for DO prediction in low-impacted rivers, while they may not be appropriate for DO modelling for highly polluted rivers. According to the obtained results, it is clearly shown that the MLPNN models performed best at two rivers (Wubu and Tributary of Huaxi River) and the ELM model performed best at the two other rivers (Huaxi and Yipin). Additionally, it was observed that the best accuracy obtained using MLPNN and ELM models differs widely from river to river, and it is sometimes difficult to select the best architecture among the nine input combinations. For example, at Wubu River the best accuracy using the MLPNN model was achieved using MLPNN4, while ELM1 performed better. At Yipin River, MLPNN6 performed better and ELM6 provided the best accuracy. Similarly, at the Huaxi River, the best accuracy was achieved using ELM2 and MLPNN2, respectively. Finally, at the tributary of the Huaxi River, MLPNN8 yielded higher accuracy, while the best accuracy was obtained using the ELM6 model. These statements reveal that, although the models used the same input variables at the four rivers, the effect of each independent water quality variable on DO concentrations differs from one river to another.

**Table 4** | Performances of different models in modelling DO at Wubu River

| | Training | | | | Validation | | | |
|---|---|---|---|---|---|---|---|---|
| **Models** | ***R*** | ***d*** | ***RMSE*** | ***MAE*** | ***R*** | ***d*** | ***RMSE*** | ***MAE*** |
| MLPNN1 | 0.998 | 0.999 | 0.061 | 0.044 | 0.885 | 0.937 | 0.554 | 0.477 |
| MLPNN2 | 0.994 | 0.997 | 0.105 | 0.079 | 0.917 | 0.943 | 0.560 | 0.422 |
| MLPNN3 | 0.930 | 0.960 | 0.391 | 0.281 | 0.845 | 0.897 | 0.783 | 0.605 |
| MLPNN4 | 0.984 | 0.991 | 0.178 | 0.134 | 0.937 | 0.968 | 0.365 | 0.262 |
| MLPNN5 | 0.897 | 0.940 | 0.439 | 0.354 | 0.542 | 0.729 | 1.137 | 0.942 |
| MLPNN6 | 0.992 | 0.996 | 0.121 | 0.090 | 0.878 | 0.932 | 0.586 | 0.387 |
| MLPNN7 | 0.974 | 0.986 | 0.227 | 0.161 | 0.880 | 0.928 | 0.577 | 0.485 |
| MLPNN8 | 0.962 | 0.980 | 0.266 | 0.206 | 0.929 | 0.961 | 0.431 | 0.341 |
| MLPNN9 | 0.954 | 0.976 | 0.294 | 0.226 | 0.723 | 0.860 | 0.793 | 0.513 |
| ELM1 | 0.826 | 0.898 | 0.553 | 0.446 | 0.918 | 0.953 | 0.418 | 0.322 |
| ELM2 | 0.854 | 0.916 | 0.511 | 0.420 | 0.832 | 0.890 | 0.586 | 0.421 |
| ELM3 | 0.609 | 0.733 | 0.778 | 0.592 | 0.647 | 0.766 | 0.793 | 0.675 |
| ELM4 | 0.791 | 0.874 | 0.600 | 0.508 | 0.870 | 0.923 | 0.518 | 0.359 |
| ELM5 | 0.620 | 0.742 | 0.769 | 0.631 | 0.698 | 0.828 | 0.753 | 0.653 |
| ELM6 | 0.821 | 0.894 | 0.559 | 0.453 | 0.916 | 0.944 | 0.439 | 0.326 |
| ELM7 | 0.761 | 0.852 | 0.636 | 0.535 | 0.862 | 0.925 | 0.526 | 0.391 |
| ELM8 | 0.856 | 0.918 | 0.507 | 0.430 | 0.893 | 0.945 | 0.472 | 0.357 |
| ELM9 | 0.859 | 0.920 | 0.503 | 0.384 | 0.824 | 0.905 | 0.632 | 0.473 |

**Table 5** | Performances of different models in modelling DO at Yipin River

| | Training | | | | Validation | | | |
|---|---|---|---|---|---|---|---|---|
| **Models** | ***R*** | ***d*** | ***RMSE*** | ***MAE*** | ***R*** | ***d*** | ***RMSE*** | ***MAE*** |
| MLPNN1 | 0.999 | 0.999 | 0.050 | 0.036 | 0.677 | 0.843 | 0.929 | 0.711 |
| MLPNN2 | 0.947 | 0.975 | 0.352 | 0.270 | 0.768 | 0.887 | 0.752 | 0.583 |
| MLPNN3 | 0.861 | 0.897 | 0.564 | 0.426 | 0.274 | 0.587 | 1.216 | 1.045 |
| MLPNN4 | 0.976 | 0.988 | 0.237 | 0.176 | 0.693 | 0.850 | 0.861 | 0.670 |
| MLPNN5 | 0.845 | 0.861 | 0.588 | 0.421 | 0.355 | 0.688 | 1.136 | 0.866 |
| MLPNN6 | 0.958 | 0.977 | 0.315 | 0.239 | 0.824 | 0.906 | 0.656 | 0.536 |
| MLPNN7 | 0.963 | 0.976 | 0.298 | 0.238 | 0.719 | 0.863 | 0.829 | 0.654 |
| MLPNN8 | 0.938 | 0.960 | 0.379 | 0.288 | 0.789 | 0.896 | 0.746 | 0.584 |
| MLPNN9 | 0.916 | 0.958 | 0.441 | 0.348 | 0.717 | 0.865 | 0.821 | 0.606 |
| ELM1 | 0.831 | 0.926 | 0.609 | 0.488 | 0.654 | 0.823 | 0.893 | 0.722 |
| ELM2 | 0.858 | 0.923 | 0.562 | 0.433 | 0.701 | 0.851 | 0.840 | 0.627 |
| ELM3 | 0.431 | 0.419 | 0.989 | 0.813 | 0.409 | 0.567 | 0.966 | 0.709 |
| ELM4 | 0.855 | 0.916 | 0.568 | 0.451 | 0.686 | 0.850 | 0.796 | 0.584 |
| ELM5 | 0.505 | 0.443 | 0.946 | 0.752 | 0.270 | 0.579 | 1.061 | 0.810 |
| ELM6 | 0.856 | 0.934 | 0.567 | 0.437 | 0.828 | 0.913 | 0.600 | 0.481 |
| ELM7 | 0.873 | 0.920 | 0.535 | 0.420 | 0.714 | 0.860 | 0.784 | 0.624 |
| ELM8 | 0.864 | 0.921 | 0.551 | 0.434 | 0.781 | 0.884 | 0.660 | 0.510 |
| ELM9 | 0.837 | 0.922 | 0.600 | 0.492 | 0.731 | 0.865 | 0.727 | 0.576 |

**Table 6** | Performances of different models in modelling DO at Huaxi River

| | Training | | | | Validation | | | |
|---|---|---|---|---|---|---|---|---|
| **Models** | ***R*** | ***d*** | ***RMSE*** | ***MAE*** | ***R*** | ***d*** | ***RMSE*** | ***MAE*** |
| MLPNN1 | 0.928 | 0.975 | 0.441 | 0.315 | 0.603 | 0.815 | 1.063 | 0.915 |
| MLPNN2 | 0.816 | 0.926 | 0.680 | 0.454 | 0.687 | 0.855 | 0.967 | 0.675 |
| MLPNN3 | 0.985 | 0.993 | 0.202 | 0.138 | 0.224 | 0.600 | 1.535 | 1.281 |
| MLPNN4 | 0.838 | 0.921 | 0.641 | 0.493 | 0.653 | 0.834 | 0.966 | 0.786 |
| MLPNN5 | 0.850 | 0.934 | 0.618 | 0.472 | 0.107 | 0.580 | 1.461 | 1.120 |
| MLPNN6 | 0.860 | 0.926 | 0.607 | 0.446 | 0.672 | 0.839 | 0.946 | 0.706 |
| MLPNN7 | 0.877 | 0.931 | 0.570 | 0.424 | 0.687 | 0.843 | 1.105 | 0.851 |
| MLPNN8 | 0.728 | 0.848 | 0.805 | 0.536 | 0.662 | 0.836 | 1.024 | 0.777 |
| MLPNN9 | 0.797 | 0.901 | 0.710 | 0.465 | 0.495 | 0.743 | 1.161 | 0.827 |
| ELM1 | 0.725 | 0.832 | 0.809 | 0.628 | 0.684 | 0.838 | 0.903 | 0.718 |
| ELM2 | 0.637 | 0.767 | 0.905 | 0.663 | 0.757 | 0.857 | 0.815 | 0.605 |
| ELM3 | 0.683 | 0.828 | 0.858 | 0.655 | 0.466 | 0.734 | 1.117 | 0.881 |
| ELM4 | 0.733 | 0.849 | 0.799 | 0.587 | 0.708 | 0.859 | 0.888 | 0.678 |
| ELM5 | 0.571 | 0.722 | 0.964 | 0.729 | 0.627 | 0.713 | 1.009 | 0.793 |
| ELM6 | 0.737 | 0.860 | 0.793 | 0.628 | 0.622 | 0.819 | 1.032 | 0.743 |
| ELM7 | 0.664 | 0.808 | 0.878 | 0.680 | 0.727 | 0.844 | 0.865 | 0.685 |
| ELM8 | 0.688 | 0.816 | 0.852 | 0.612 | 0.633 | 0.800 | 0.959 | 0.764 |
| ELM9 | 0.539 | 0.692 | 0.989 | 0.697 | 0.663 | 0.792 | 0.928 | 0.761 |

**Table 7** | Performances of different models in modelling DO at Tributary of Huaxi River

| | Training | | | | Validation | | | |
|---|---|---|---|---|---|---|---|---|
| **Models** | ***R*** | ***d*** | ***RMSE*** | ***MAE*** | ***R*** | ***d*** | ***RMSE*** | ***MAE*** |
| MLPNN1 | 0.823 | 0.902 | 1.058 | 0.717 | 0.447 | 0.692 | 1.494 | 1.122 |
| MLPNN2 | 0.979 | 0.988 | 0.377 | 0.293 | 0.387 | 0.663 | 1.855 | 1.360 |
| MLPNN3 | 0.990 | 0.995 | 0.262 | 0.190 | 0.196 | 0.460 | 2.808 | 2.351 |
| MLPNN4 | 0.916 | 0.946 | 0.747 | 0.572 | 0.566 | 0.756 | 1.365 | 1.019 |
| MLPNN5 | 0.987 | 0.993 | 0.294 | 0.210 | 0.571 | 0.718 | 2.054 | 1.506 |
| MLPNN6 | 0.878 | 0.930 | 0.867 | 0.630 | 0.549 | 0.766 | 1.525 | 1.161 |
| MLPNN7 | 0.895 | 0.937 | 0.815 | 0.622 | 0.347 | 0.544 | 2.008 | 1.450 |
| MLPNN8 | 0.964 | 0.981 | 0.480 | 0.343 | 0.649 | 0.765 | 1.984 | 1.535 |
| MLPNN9 | 0.951 | 0.973 | 0.564 | 0.423 | 0.564 | 0.471 | 4.494 | 3.542 |
| ELM1 | 0.649 | 0.761 | 1.374 | 1.136 | 0.351 | 0.629 | 1.532 | 1.292 |
| ELM2 | 0.636 | 0.752 | 1.393 | 1.142 | 0.235 | 0.545 | 1.643 | 1.286 |
| ELM3 | 0.563 | 0.665 | 1.492 | 1.167 | 0.139 | 0.456 | 1.752 | 1.483 |
| ELM4 | 0.607 | 0.722 | 1.436 | 1.176 | 0.212 | 0.561 | 1.692 | 1.327 |
| ELM5 | 0.651 | 0.764 | 1.371 | 1.061 | 0.359 | 0.647 | 1.563 | 1.197 |
| ELM6 | 0.719 | 0.820 | 1.256 | 0.971 | 0.400 | 0.631 | 1.481 | 1.197 |
| ELM7 | 0.613 | 0.734 | 1.426 | 1.157 | 0.146 | 0.454 | 1.643 | 1.398 |
| ELM8 | 0.609 | 0.731 | 1.432 | 1.119 | 0.238 | 0.509 | 1.576 | 1.276 |
| ELM9 | 0.608 | 0.725 | 1.434 | 1.194 | 0.313 | 0.493 | 1.529 | 1.304 |

Estimated DO concentrations at the Wubu River using the ELM and MLPNN models are shown in Table 4. In the following, a more detailed evaluation for each of the different models is provided and several main points are highlighted. First, in the training phase, the MLPNN models worked very well and provided high accuracy for all input combinations compared to the ELM models. DO concentrations were better fitted to the measured values using MLPNN with $R$ and $d$ ranging from 0.897 to 0.998 and 0.940 to 0.999, respectively, compared to the ELM models which supplied values of $R$ and $d$ ranging from 0.609 to 0.859 and 0.733 to 0.920, respectively. Second, the best accuracy in the training phase was obtained using MLPNN1, while the best accuracy for ELM models was obtained using the ELM9 model. This statement leads to the conclusion that the influence of the different water quality variables on the estimation of DO in rivers during model calibration is not as similar, and the MLPNN models that benefit from training times higher than the ELM models are capable of capturing the non-linear relationships between water quality variables and DO concentrations. By comparing the performances of the MLPNN and ELM models during the validation phase, it is clear that for the MLPNN models, the best results were achieved using the MLPNN4 model ($R = 0.937$, $d = 0.968$) with five water quality variables, TE, pH, EC, $NH_3$-N and TP, as inputs. Significant variability was observed between the nine developed models. $R$ and $d$ ranged from 0.542 to 0.937 and 0.860 to 0.968, with an average of 0.837 and 0.906, respectively. Although MLPNN4 is the best model, MLPNN2, MLPNN4 and MLPNN8 showed relatively similar results and MLPNN4 is slightly better than MLPNN2 and MLPNN8 when focusing only on the $R$ and $d$ values. However, when comparing the three models based on the error indices (*RMSE* and *MAE*), MLPNN4 performed much better than the other two models. Regarding the remaining set of models, it is clear from Table 4 that MLPNN1, MLPNN3, MLPNN6 and MLPNN7 showed relatively similar results, with average $R$ values of 0.872 and average $d$ values of 0.923, respectively, and performed better when compared to the MLPNN5 and MLPNN9 models. Finally, the MLPNN5 model performs worst compared to all the other developed models ($RMSE = 1.137$ mg/L, $MAE = 0.942$ mg/L, $R = 0.542$, $d = 0.729$). However, the MLPNN5 model would have the worst performance for DO estimation because the TE variable is removed from the input variables. MLPNN9 that uses fewer input variables (three inputs), may have the same problem, but suffers less than MLPNN5, because TE is included accompanied by the PI and EC variables.

Estimated DO at Yipin River using the ELM and MLPNN models is shown in Table 5. At first glance, the two models MLPNN and ELM provided low accuracy compared to the performances obtained at the Wubu River. For the MLPNN models, $R$ values range from 0.274 to 0.824 and $d$ values range from 0.587 to 0.906. Similarly, for the ELM models, $R$ values range from 0.270 to 0.828 and $d$ values range from 0.579 to 0.913. In the validation phase, the average $R$ and $d$ values using the MLPNN models were 0.646 and 0.821, respectively, while the average values of the same indices for the ELM models were 0.642 and 0.799, respectively. MLPNN3 gives the worst performances with the highest *RMSE* and *MAE*, and lowest $R$ and $d$, among the nine models. Regarding the ELM models, ELM5 gives the worst performances among the nine ELM models. For overall comparison, ELM6 was the most predictive model and performed slightly better than the MLPNN6 model. For numerical comparison between the best two models, ELM6 yielded a high and best improvement of the MLPNN6, improving its accuracy by increasing the values of the $R$ and $d$ by 0.4% and 0.7%, respectively, and decreasing the values of the *RMSE* and *MAE* by 8.53%, and 10.26%, respectively.

The summary of statistical indices of the training and validation data in prediction of DO using ELM and MLPNN models at the Huaxi River are presented in Table 6. According to the obtained results, it is clear that the two models performed less well than for the two previous rivers (Wubu and Yipin), and this leads to an informed judgement: increases in pollution level associated with low level of DO concentrations in the river results in the models being unable to correctly capture the relationship between DO and water quality variables. The $R$ and $d$ values of MLPNN models ranged between 0.107 and 0.687 and 0.580 and 0.855, with average values of 0.532 and 0.771, respectively. Similarly, the $R$ and $d$ values of ELM models ranged between 0.466 and 0.757 and 0.713 and 0.857, with average values of 0.654 and 0.806, respectively. Overall, the ELM models performed better

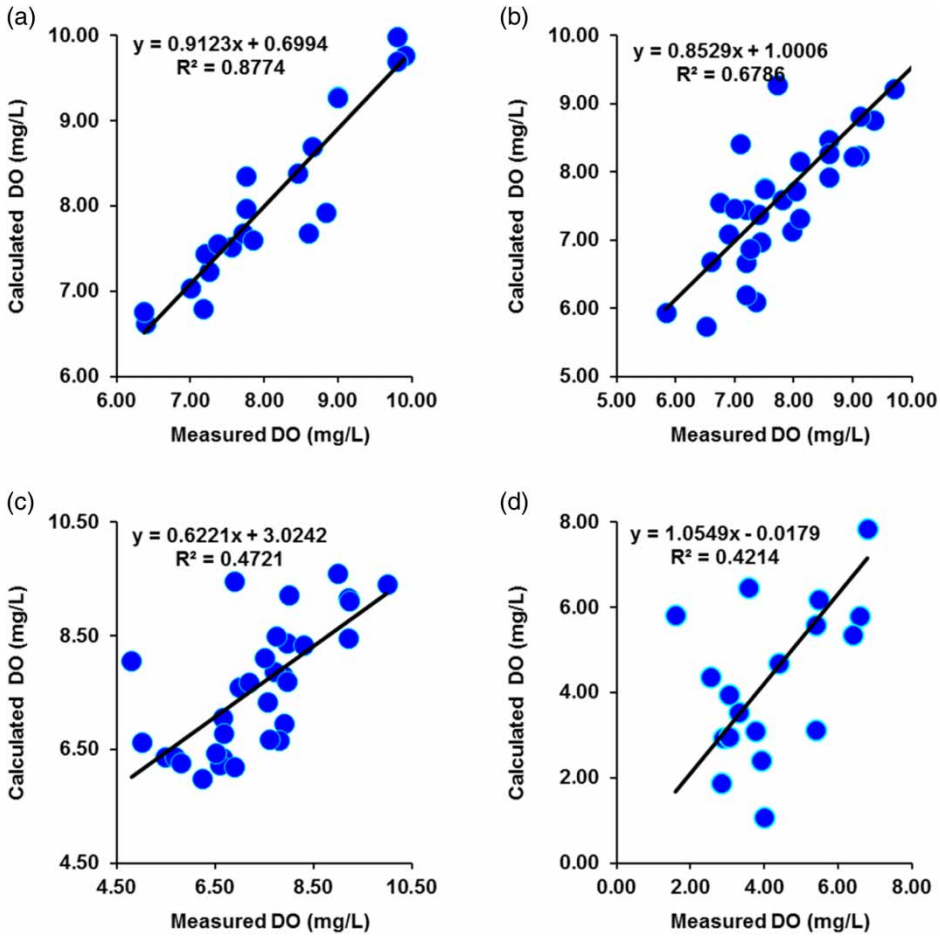


**Figure 2** | Scatterplots of predicted versus measured values of dissolved oxygen (DO) concentration using the best MLPNN models in the validation phase for: (a) Wubu River, (b) Yipin River, (c) Huaxi River and (d) Tributary of Huaxi River.

compared to the MLPNN models. At Huaxi River, the ELM2 model provides better DO estimates than the MLPNN2, and the results indicate that DO can be predicted with $R$ and $d$ values equal to 0.757 and 0.857 ($RMSE =$ 0.815 mg/L, $MAE = 0.605$ mg/L), respectively, which are higher than the values obtained using the MLPNN2 model. According to Legates & McCabe (1999) and Moriasi *et al.* (2007), values of $R$ greater than 0.70 are considered acceptable; consequently, none of the nine MLPNN models' results are acceptable.

Training and validation results of the ELM and MLPNN models at the tributary of Huaxi River are presented in Table 7. Models' performances were generally unsatisfactory for all nine input combinations according to the guidelines from Legates & McCabe (1999) and Moriasi *et al.* (2007). Although the performances of the MLPNN models in the training phase were very satisfactory, the models performed poorly during the validation phase. As is shown in Table 7, the average values of $R$ and $d$ for the MLPNN models during the validation phase were 0.475 and 0.648, respectively, while for the ELM models the values of the two indices dropped to 0.266 and 0.547, with 20% and 10% reduction, respectively. There are several potential factors that could impact the accuracy of the models at this specific site. First, the low correlation coefficient between DO and TE certainly has a great influence. Second, the accuracy of the models decreased dramatically with the increase of the pollution level in the studied rivers, and it is difficult for the models to consider the impact of anthropogenic influences in highly polluted rivers. Measured and predicted DO concentrations with MLPNN and ELM models in the four rivers in the validation phase are presented in Figures 2 and 3.

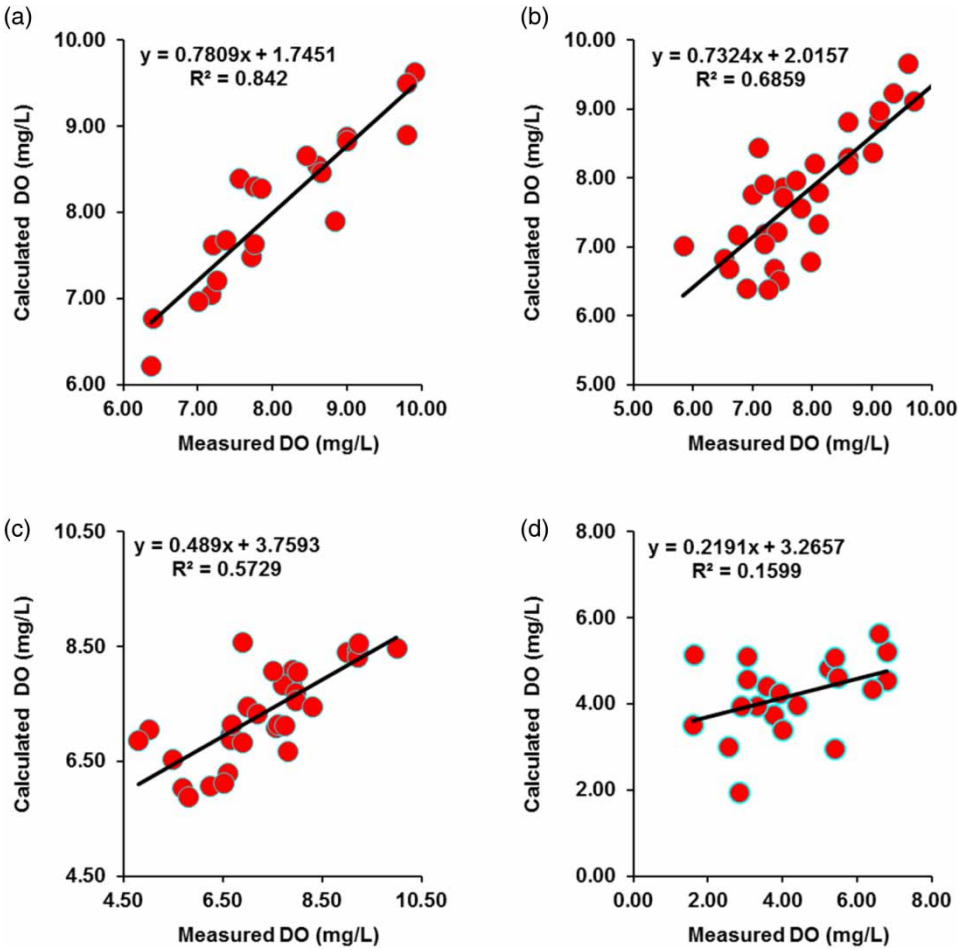


**Figure 3** | Scatterplots of predicted versus measured values of dissolved oxygen (DO) concentration using the best ELM models in the validation phase for: (a) Wubu River, (b) Yipin River, (c) Huaxi River and (d) Tributary of Huaxi River.

## CONCLUSIONS

In this study, ELM and MLPNN models were implemented to predict the DO concentrations using the daily observed river temperature, pH, PI, $NH_3$-N, EC, COD, TN and TP for four urban rivers in the backwater zone of the TGR. Model results showed that the ELM and MLPNN models perform well for the Wubu River, acceptably for the Yipin River, moderately for the Huaxi River, and poorly for the Tributary of Huaxi River in DO prediction, and model performance is negatively correlated with pollution level in each river. It can be concluded that MLPNN and ELM models can be applied for DO prediction in low-impacted rivers, while they may not be appropriate for DO modelling for highly polluted rivers since it is difficult for these models to consider the impact of anthropogenic influences.

## ACKNOWLEDGEMENTS

This work was jointly funded by the National Key R&D Program of China (2018YFC0407200), China Postdoctoral Science Foundation (2018M640499), and the research project from Nanjing Hydraulic Research Institute (Y118009). The authors acknowledge Chongqing Environment Protection Bureau for providing the water quality data used in this manuscript.

## REFERENCES


Altunkaynak, A., Özger, M. & Çakmakci, M. 2005 Fuzzy logic modeling of the dissolved oxygen fluctuations in Golden Horn. *Ecological Modelling* **189** (3–4), 436–446.

Antanasijević, D., Pocajt, V., Povrenović, D., Perić-Grujić, A. & Ristić, M. 2013 Modelling of dissolved oxygen content using artificial neural networks: Danube River, North Serbia, case study. *Environmental Science and Pollution Research* **20** (12), 9006–9013.

Ay, M. & Kisi, O. 2012 Modeling of dissolved oxygen concentration using different neural network techniques in Foundation Creek, El Paso County, Colorado. *ASCE Journal of Environmental Engineering* **138**, 6.

Ay, M. & Kişi, Ö. 2017 Estimation of dissolved oxygen by using neural networks and neuro fuzzy computing techniques. *KSCE Journal of Civil Engineering* **21** (5), 1631–1639.

Branco, P., Santos, J. M., Amaral, S., Romão, F., Pinheiro, A. N. & Ferreira, M. T. 2016 Potamodromous fish movements under multiple stressors: connectivity reduction and oxygen depletion. *Science of the Total Environment* **572**, 520–525.

Chen, D., Lu, J. & Shen, Y. 2010 Artificial neural network modelling of concentrations of nitrogen, phosphorus and dissolved oxygen in a non-point source polluted river in Zhejiang Province, southeast China. *Hydrological Processes* **24** (3), 290–299.

Cho, J. & Ha, S. R. 2010 Parameter optimization of the QUAL2 K model for a multiple-reach river using an influence coefficient algorithm. *Science of the Total Environment* **408** (8), 1985–1991.

Cox, B. A. 2003 A review of currently available in-stream water-quality models and their applicability for simulating dissolved oxygen in lowland rivers. *Science of the Total Environment* **314–316**, 335–377.

Csábrági, A., Molnár, S., Tanos, P. & Kovács, J. 2017 Application of artificial neural networks to the forecasting of dissolved oxygen content in the Hungarian section of the river Danube. *Ecological Engineering* **100**, 63–72.

Diamantopoulou, M. J., Antonopoulos, V. Z. & Papamichail, D. M. 2007 Cascade correlation artificial neural networks for estimating missing monthly values of water quality parameters in rivers. *Water Resources Management* **21** (3), 649–662.

Du, B., Hauck, L. M. & Saleh, A. 2008 Using QUAL2 K to investigate dissolved oxygen for Upper Oyster Creek, Texas. Century Watershed Technology: Improving Water Quality and Environment Conference Proceedings, Concepcion, Chile.

Giusti, E. & Marsili-Libelli, S. 2009 Spatio-temporal dissolved oxygen dynamics in the Orbetello lagoon by fuzzy pattern recognition. *Ecological Modelling* **220** (19), 2415–2426.

Haykin, S. 1999 *Neural Networks: A Comprehensive Foundation*. Prentice Hall, Upper Saddle River, NJ, USA.

Heddam, S. 2014a Generalized regression neural network-based approach for modelling hourly dissolved oxygen concentration in the Upper Klamath River, Oregon, USA. *Environmental Technology* **35** (13), 1650–1657.

Heddam, S. 2014b Modelling hourly dissolved oxygen concentration (DO) using dynamic evolving neural-fuzzy inference system (DENFIS)-based approach: case study of Klamath River at Miller Island Boat Ramp, OR, USA. *Environmental Science and Pollution Research* **21** (15), 9212–9227.

Heddam, S. 2016 Use of optimally pruned extreme learning machine (OP-ELM) in forecasting dissolved oxygen concentration (DO) several hours in advance: a case study from the Klamath River, Oregon, USA. *Environmental Processes* **3** (4), 909–937.

Heddam, S. & Kisi, O. 2017 Extreme learning machines: a new approach for modeling dissolved oxygen (DO) concentration with and without water quality variables as predictors. *Environmental Science and Pollution Research* **24** (20), 16702–16724.

Heddam, S. & Kisi, O. 2018 Modelling daily dissolved oxygen concentration using least square support vector machine, multivariate adaptive regression splines and M5 model tree. *Journal of Hydrology* **559**, 499–509.

Hornik, K. 1991 Approximation capabilities of multilayer feedforward networks. *Neural Networks* **4** (2), 251–257.

Hornik, K., Stinchcombe, M. & White, H. 1989 Multilayer feedforward networks are universal approximators. *Neural Networks* **2** (5), 359–366.

Huang, G. B., Chen, L. & Siew, C. K. 2006a Universal approximation using incremental constructive feedforward networks with random hidden nodes. *IEEE Transactions on Neural Networks* **17** (4), 879–892.

Huang, G. B., Zhu, Q. & Siew, C. 2006b Extreme learning machine: theory and applications. *Neurocomputing* **70** (1–3), 489–501.

Ji, X., Shang, X., Dahlgren, R. A. & Zhang, M. 2017 Prediction of dissolved oxygen concentration in hypoxic river systems using support vector machine: a case study of Wen-Rui Tang River, China. *Environmental Science and Pollution Research* **24** (19), 16062–16076.

Kannel, P. R., Kanel, S. R., Lee, S., Lee, Y. & Gan, T. Y. 2010 A review of public domain water quality models for simulating dissolved oxygen in rivers and streams. *Environmental Modeling & Assessment* **16** (2), 183–204.

Keshtegar, B. & Heddam, S. 2017 Modeling daily dissolved oxygen concentration using modified response surface method and artificial neural network: a comparative study. *Neural Computing & Applications* **30**, 2995–3006.

Legates, D. R. & McCabe, G. J. 1999 Evaluating the use of 'goodness-of-fit' measures in hydrologic and hydroclimatic model validation. *Water Resources Research* **35** (1), 233–241.

Li, W., Yang, M., Liang, Z., Zhu, Y., Mao, W., Shi, J. & Chen, Y. 2013 Assessment for surface water quality in Lake Taihu Tiaoxi River Basin China based on support vector machine. *Stochastic Environmental Research and Risk Assessment* **27** (8), 1861–1870.

Liu, S., Xu, L., Li, D., Li, Q., Jiang, Y., Tai, H. & Zeng, L. 2013 Prediction of dissolved oxygen content in river crab culture based on least squares support vector regression optimized by improved particle swarm optimization. *Computers and Electronics in Agriculture* **95**, 82–91.

Meding, M. E. & Jackson, L. J. 2003 Biotic, chemical, and morphometric factors contributing to winter anoxia in prairie lakes. *Limnology and Oceanography* **48** (4), 1633–1642.

Moriasi, D. N., Arnold, J. G., Van Liew, M. W., Bingner, R. L., Harmel, R. D. & Veith, T. L. 2007 Model evaluation guidelines for systematic quantification of accuracy in watershed simulations. *Transactions of the ASABE* **50** (3), 885–900.

Najah, A., El-Shafie, A., Karim, O. A. & El-Shafie, A. H. 2014 Performance of ANFIS versus MLPNN dissolved oxygen prediction models in water quality monitoring. *Environmental Science and Pollution Research* **21** (3), 1658–1670.

Olden, J. D. & Jackson, D. A. 2002 Illuminating the 'black box': a randomization approach for understanding variable contributions in artificial neural networks. *Ecological Modelling* **154** (1–2), 135–150.

Palmieri, V. & Carvalho, R. J. D. 2006 Qual2e model for the Corumbataí River. *Ecological Modelling* **198** (1), 269–275.

Poulson, S. R. & Sullivan, A. B. 2010 Assessment of diel chemical and isotopic techniques to investigate biogeochemical cycles in the upper Klamath River, Oregon, USA. *Chemical Geology* **269** (3–4), 3–11.

Robarts, R. D., Waiser, M. J., Arts, M. T. & Evans, M. S. 2005 Seasonal and diel changes of dissolved oxygen in a hypertrophic prairie lake. *Lakes & Reservoirs: Research & Management* **10** (3), 167–177.

Rumelhart, D. E., Hinton, G. E. & Williams, R. J. 1986 Learning internal representations by error propagation. In: *Parallel Distributed Processing: Explorations in the Microstructure of Cognition. Foundations*, Vol. I (D. E. Rumelhart & P. D. P. McClelland eds). MIT Press, Cambridge, MA, USA, pp. 318–362.

Ruuhijärvi, J., Rask, M., Vesala, S., Westermark, A., Olin, M., Keskitalo, J. & Lehtovaara, A. 2010 Recovery of the fish community and changes in the lower trophic levels in a eutrophic lake after a winter kill of fish. *Hydrobiologia* **646** (1), 145–158.

Schmid, B. H. & Koskiaho, J. 2006 Artificial neural network modeling of dissolved oxygen in a wetland pond: the case of Hovi, Finland. *Journal of Hydrologic Engineering* **11** (2), 188–192.

Singh, K. P., Basant, A., Malik, A. & Jain, G. 2009 Artificial neural network modeling of the river water quality-a case study. *Ecological Modelling* **220** (6), 888–895.

Soyupak, S., Karaer, F., Gürbüz, H., Kivrak, E., Sentürket, E. & Yazici, A. 2003 A neural network-based approach for calculating dissolved oxygen profiles in reservoirs. *Neural Computing & Applications* **12** (3–4), 166–172.

Wang, Y., Liao, M., Sun, G. & Gong, J. 2005 Analysis of the water volume, length, total area and inundated area of the Three Gorges Reservoir, China using the SRTM DEM data. *International Journal of Remote Sensing* **26** (18), 4001–4012.

Wei, Y., Xiao, G., Deng, H., Chen, H., Tong, M., Zhao, G. & Liu, Q. 2015 Hyperspectral image classification using FPCA-based kernel extreme learning machine. *Optik* **126** (23), 3942–3948.

Wen, X., Fang, J., Diao, M. & Zhang, C. 2013 Artificial neural network modeling of dissolved oxygen in the Heihe River, Northwestern China. *Environmental Monitoring and Assessment* **185** (5), 4361–4371.

Wetzel, R. G. 2001 *Limnology: Lake and River Ecosystems*. Academic Press, San Diego, CA, USA.

Yan, C., Qi, J., Ma, J., Tang, H., Zhang, T. & Li, H. 2017 Determination of carbon and sulfur content in coal by laser induced breakdown spectroscopy combined with kernel-based extreme learning machine. *Chemometrics and Intelligent Laboratory Systems* **167**, 226–231.

Yang, C., Chen, C. & Lee, C. 2011 Comprehensive river water quality management by simulation and optimization models. *Environmental Modeling & Assessment* **16**, 283–294.

Zhang, Y., Wang, Y., Zhou, G., Jin, J., Wang, B., Wang, X. & Cichocki, A. 2018 Multi-kernel extreme learning machine for EEG classification in brain-computer interfaces. *Expert Systems with Applications* **96**, 302–310.

Zhu, S., Mostafaei, A., Luo, W., Jia, B. & Dai, J. 2018 Assessing water quality for urban tributaries of the Three Gorges Reservoir. *China. Journal of Water Reuse and Desalination* **9** (1), 105–114.

Zounemat-Kermani, M. & Scholz, M. 2014 Modeling of dissolved oxygen applying stepwise regression and a template-based fuzzy logic system. *Journal of Environmental Engineering* **140** (1), 69–76.

First received 25 November 2018; accepted in revised form 2 July 2019. Available online 29 July 2019